Implementation of a Boundary Element Method for High Frequency Scattering by Convex Polygons with Impedance Boundary Conditions

Mosiamisi Mokgolele

Botswana University of Agriculture and Natural Resoures, Private Bag 0027, Gaborone, Botswana.

Many acoustic and electromagnetic wave scattering problems can be formulated as the Helmholtz equation. Standard finite and boundary element method solution of these problems becomes expensive, as the frequency of incident wave increases. On going research has been devoted to finding methods that do not loose robustness when the wave number increases. Recently, Chandler-Wilde et al. have proposed a novel Galerkin boundary element method to solve the problem of acoustic scattering by a convex polygon with impedance boundary conditions. They applied approximation spaces consisting of piecewise polynomials supported on a graded mesh with smaller elements adjacent to the corners of the polygon and multiplied by plane wave basis functions. They demonstrated via rigorous error analysis that was supported by numerical experiments that the number of degrees of freedom required to achieve a prescribed level of accuracy need only grow logarithmically as frequency increases. In this paper, we discuss issues related to detail implementation of their numerical method.

1. INTRODUCTION

We consider the two-dimensional problem of scattering of a time-harmonic acoustic incident plane wave:

$$u^i(\mathbf{x}) = e^{ik\mathbf{x}\cdot\mathbf{d}}, \text{ in } D := \mathbb{R}^2\backslash\bar{\Omega}; \tag{1}$$

by a convex polygon Ω, with impedance boundary Γ. Here $\mathbf{x} = (x_1, x_2) \in \mathbb{R}^2$, $\mathbf{d} = (\sin\theta, -\cos\theta) \in \mathbb{R}^2$ is a unit vector representing the direction of the incident field, θ is the incidence angle, and the frequency of the incident wave is proportional to the wavenumber $k > 0$. The scattered field $u^s := u^t - u^i \in C^2(\bar{D})$ (where u^t and u^i denote the total and incident field respectively) satisfies the Helmholtz equation:

$$\Delta u^s + k^2 u^s = 0, \text{ in } D. \tag{2}$$

We shall consider the impedance boundary condition here:

$$\frac{\partial u^t}{\partial \mathbf{n}} + ik\beta u^t = 0, \text{ on } \Gamma; \tag{3}$$

(where $\mathbf{n} = (n_1, n_2)$ denotes the outward unit normal vector to Γ, as depicted in Fig. 1 and $\beta \in L^\infty(\Gamma)$ and $\text{Re}\beta > 0$ is relative surface admittance), and is supplemented with the Sommerfeld radiation condition:

$$\lim_{r\to\infty} r^{\frac{1}{2}} \left(\frac{\partial u^s}{\partial r} - iku^s \right) = 0; \tag{4}$$

where $r := |\mathbf{x}|$ and the limit holds uniformly in $\mathbf{x}/|\mathbf{x}|$. The Sommerfeld radiation condition is essential to scattering problems because it ensures that the scattered field is not reflected back from infinity.

As k increases, the incident field oscillates more rapidly, and so the complexity of the solution of Eq.(2) increases. As a result, the computational cost of standard schemes, such as the finite element or boundary element methods will grow in direct proportion to k, leading to large computing times for large k. It has been shown that in order to accurately model a wave, a fixed number of degrees of freedom M are needed per wavelength, with a rule of thumb in the engineering literature of 6 to 10 degrees of freedom per wavelength needed to maintain accuracy.[1,2] The price to pay for fixing M is that the number of degrees of freedom will be proportional to $(kL)^{d-1}$ in case of boundary element methods, where L is the linear dimension of the scattering obstacle and $d = 2$ or 3 is the dimension of the problem. Thus, as either k or the size of the scatterer grows, so does the number of degrees of freedom (at least $\mathcal{O}(k)$) in two-dimensional, hence the computational cost of numerical schemes increases. The previous and the current development on this active field of scattering problems is outlined explicitly at length in.[3]

For this paper we begin in Section 2 by discussing the boundary integral method we are going to apply. We describe the approximation space for the problem in Section 3. We proceed in Section 4 by presenting the implementation of our Galerkin scheme. We present formulas for the Galerkin scheme and describe how to evaluate oscillatory and non oscillatory integrals. In Section 5, we discuss how to solve non-overlapping integrals, a detail explanation of Gaussian quadrature rule is also explained in this section. In Section 6 we choose an example for our numerical experiment and present some results, whereas most of them can be found in.[4,5] We discuss our conclusion and some recommendations in Section 7.

2. BOUNDARY INTEGRAL EQUATION METHOD

The boundary value problem Eqs. (2) - (4) can be reformulated into boundary integral equation by applying Green's rep-
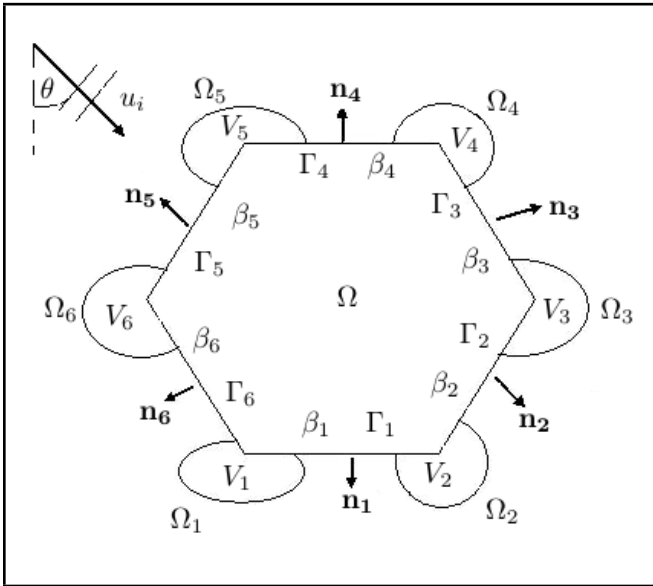
Figure 1. Scattering by an impedance convex polygon.

resentation theorems [7.12 and 9.6][6] and Green's second theorem [theorem 4.4],[6] (see also[4] for details), which leads to standard boundary integral equation for unknown u^t:

$$u^t(\mathbf{x}) - 2 \int_\Gamma \left(\frac{\partial \Phi'(\mathbf{x}, \mathbf{y})}{\partial \mathbf{n}(\mathbf{y})} + \mathrm{i}k\beta(\mathbf{y})\Phi'(\mathbf{x}, \mathbf{y}) \right) u^t(\mathbf{y})\mathrm{d}s(\mathbf{y}) =$$
$$2f(\mathbf{x}), \quad \mathbf{x} \in \Gamma; \quad (5)$$

where $\Phi'(\mathbf{x}, \mathbf{y}) := \frac{\mathrm{i}}{4} H_0^{(1)}(k|\mathbf{x} - \mathbf{y}|)$, ($H_0^{(1)}$ is the Hankel function of first kind of order zero) and $f(\mathbf{x}) = u^i(\mathbf{x})$. The integral Eq. (5) suffers from so-called spurious eigenfrequencies; that is, it is not uniquely solvable for all wavenumbers.[7,8] However, this problem is often ignored in the literature.[7] Various options exist to overcome this difficulty.[4]

We begin by defining some notations, see Fig. 1. We write the boundary of the polygon as $\Gamma = \cup_{j=1}^{n_s}\Gamma_j$, where Γ_j, $j = 1, \ldots, n_s$ are the n_s^{th} sides of the polygon, ordered so that Γ_j, $j = 1, \ldots, n_{sh}$, are in shadow, and Γ_j, $j = n_{sh} + 1, \ldots, n_s$ are illuminated, with j increasing anticlockwise, as shown in Fig. 1.

We denote the corners of the polygon by V_j, $j = 1, \ldots, n_s$, and set $V_{n_s+1} = V_1$, so that for $j = 1, \ldots, n_s$, Γ_j is the line joining V_j with V_{j+1}. We denote the length of Γ_j by $L_j = |V_{j+1} - V_j|$, the external angle at each vertex V_j by $\Omega_j \in (\pi, 2\pi)$, the unit normal vector to Γ_j by $\mathbf{n}_j$, and the angle of the incident plane wave, as measured anticlockwise from the downward vertical, by $\theta \in [0, 2\pi)$. We represent $\mathbf{x} \in \Gamma$ parametrically by:

$$\mathbf{x}(s) = V_j + \left(s - \sum_{n=1}^{j-1} L_{n_s} \right)\left(\frac{V_{j+1} - V_j}{L_j} \right);$$
$$\text{for } s \in \left(\sum_{n=1}^{j-1} L_{n_s}, \sum_{n=1}^{j} L_n \right), \ j = 1, \ldots, n_s. \quad (6)$$

Define

$$\mathbf{x}(s) = (x_1(s), x_2(s)) = \{(e_l s + g_l), (f_l s + h_l)\};$$
$$\mathbf{x}(t) = (x_1(t), x_2(t)) = \{(e_j t + g_j), (f_j t + h_j)\}; \quad (7)$$

where

$$e_j := \frac{u_{j+1} - u_j}{L_j},$$
$$f_j := \frac{v_{j+1} - v_j}{L_j},$$
$$g_j := u_j - e_j \sum_{n=1}^{j-1} L_n,$$
$$h_j := v_j - f_j \sum_{n=1}^{j-1} L_{n_s}; \quad (8)$$

here point s is in element l and point t is in element j. We can write Eq. (5) in parametric form as:

$$\phi(s) - 2 \int_0^L K(s, t)\phi(t)\mathrm{d}t = 2f(s); \quad (9)$$

where $\phi(s) = u^t(\mathbf{x}(s))$, $L = \sum_{n=1}^{j} L_{n_s}$,

$$K(s, t) := \left(\frac{\partial \Phi'(\mathbf{x}(s), \mathbf{x}(t))}{\partial \mathbf{n}(\mathbf{x}(t))} + \mathrm{i}k\beta(\mathbf{x}(t))\Phi'(\mathbf{x}(s), \mathbf{x}(t)) \right); \quad (10)$$

and $\Phi'(\mathbf{x}(s), \mathbf{x}(t)) := \frac{\mathrm{i}}{4} H_0^{(1)}(k|\mathbf{x}(s) - \mathbf{x}(t)|) = \frac{\mathrm{i}}{4} H_0^{(1)}(kR)$, here

$$R =$$
$$\sqrt{[(e_l s + g_l) - (e_j t + g_j)]^2 + [(f_l s + h_l) - (g_j t + h_j)]^2}; \quad (11)$$

and finally

$$f(s) = u^i(s) = \mathrm{e}^{\mathrm{i}k(x_1(s)\sin\theta - x_2(s)\cos\theta)} =$$
$$\mathrm{e}^{\mathrm{i}k((e_l s + g_l)\sin\theta - (f_l s + h_l)\cos\theta)}. \quad (12)$$

We know that $(n_{1j}, n_{2j}).(e_l, f_l) = 0$, which implies $n_{1j}e_l + n_{2j}f_l = 0$, which implies $n_{1j} = f_l$, $n_{2j} = -e_l$ or $n_{1j} = -f_l$, $n_{2j} = e_l$ (depending on whether the unit normal is inward or outward). Using the fact that $\frac{\partial H_0^{(1)}(z)}{\partial z} = -H_1^{(1)}(z)$, and also that $\frac{\partial}{\partial \mathbf{n}} = \mathbf{n} \cdot \nabla$, we can now evaluate the explicit formula for:

$$\frac{\partial \Phi'(\mathbf{x}(s), \mathbf{x}(t))}{\partial \mathbf{n}(\mathbf{x}(t))} =$$
$$n_{1l} \frac{\partial \Phi'(\mathbf{x}(s), \mathbf{x}(t))}{\partial x_1(t)} + n_{2l} \frac{\partial \Phi'(\mathbf{x}(s), \mathbf{x}(t))}{\partial x_2(t)} =$$
$$-\frac{\mathrm{i}k}{4} \frac{H_1^{(1)}(kR)}{R} [f_j(x_1(t) - x_1(s)) - e_j(x_2(t) - x_2(s))] =$$
$$-\frac{\mathrm{i}k}{4} \frac{H_1^{(1)}(kR)}{R}$$
$$\cdot [(e_j f_l - f_j e_l)s + f_j(g_j - g_l) + e_j(h_l - h_j)]. \quad (13)$$

Therefore,

$$K(s,t) =$$
$$-\frac{k}{4}\left\{i\frac{H_1^{(1)}(kR)}{R}\right.$$
$$[(e_j f_l - f_j e_l)s + f_j(g_j - g_l) + e_j(h_l - h_j)]$$
$$\left. + \beta H_0^{(1)}(kR)\right\}. \quad (14)$$

We know that on each side of the polygon $u^t = u^i + u^r + u^d$, where u^r is the field that would be reflected by a side Γ_j, if that side was infinitely long, and u^d represents in some sense the waves diffracted by the corners of the polygon .[9] For a straight line polygon, we know u^r explicitly, and particularly for a straight line polygon with an impedance boundary condition, $u^r(\mathbf{x}) = R_\beta(\theta')e^{ik\mathbf{x}\cdot\mathbf{d}'}$,[10] where $R_\beta(\theta')$ is the reflection coefficient that is given by a reflective angle, $R_\beta(\theta') = (\frac{\cos\theta'-\beta}{\cos\theta'+\beta})$, θ' which depends on θ and Γ_j and $\mathbf{d}' = (\sin\theta, \cos\theta)$. Since u^r is a function of the incident angle, it is only featured on the illuminated side and it is zero on the shadow side of the polygon. We define our leading order behavior:

$$\Psi(s) := \begin{cases} u^i(s) + u^r(s), & \text{in illuminated region,} \\ 0, & \text{in shadow region,} \end{cases}$$
$$= \begin{cases} 2\frac{\cos\theta'}{\cos\theta'+\beta}u^i(s), & \text{in illuminated region,} \\ 0, & \text{in shadow region,} \end{cases} \quad (15)$$

and $\Phi(s) := u^d(s)$ is viewed as the diffracted wave due to the corner of the polygon. Therefore, subtracting the leading order behavior gives:

$$\Phi(s) := \phi(s) - \Psi(s). \quad (16)$$

Substituting Eq. (16) into Eq. (9), we obtain a new second kind boundary integral equation with unknown $\Phi(s)$:

$$(I - \mathcal{K})\Phi(s) = F(s); \quad (17)$$

where $\mathcal{K}v(s) := 2\int_0^L K(s,t)v(t)\,dt$, $F(s) := 2f(s) - \Psi(s) + 2\int_0^L K(s,t)\Psi(t)\,dt$, and I is the identity operator.

3. APPROXIMATION SPACE

We begin by defining a general mesh grading on $[0, L_j]$, which is composed of a polynomial grading on $[0, \lambda]$ and a geometric grading on $[\lambda, L_j]$, where L_j is the length of the jth side, $j = 1 \ldots, n_s$ (recalling that n_s is the number of sides of a polygon) $\lambda = 2\pi/k$ is the wavelength. We now define our mesh as follows: for $L_j > \lambda > 0$, $q_j > 0$, $N = 2, 3, \ldots$, where $q_j = \frac{2\nu+3}{2\pi/\Omega_j+1}$ and ν is degree of a polynomial. The mesh $\Lambda_{N,L_j,\lambda,q_j} := \{y_0, \ldots, y_{N+N_{L_j,\lambda,q_j}}\}$ consists of the points:

$$y_i = \lambda\left(\frac{i}{N}\right)^{q_j}, \quad i = 0, \ldots, N; \quad (18)$$

$$y_{N+j} := \lambda\left(\frac{L_j}{\lambda}\right)^{j/N_{L_j,\lambda,q_j}}, \quad j = 1, \ldots, N_{L_j,\lambda,q_j}. \quad (19)$$

Where $N_{L_j,\lambda,q_j} = \lceil\hat{N}_{L_j,\lambda,q_j}\rceil$,

$$\hat{N}_{L_j,\lambda,q_j} = \frac{-\log(L_j/\lambda)}{q_j\log(1-1/N)}. \quad (20)$$

Here, $\lceil z \rceil$ denotes the smallest integer greater than or equal to z, for $z \in \mathbb{R}$. Specifically, N_{L_j,λ,q_j} is the smallest positive integer greater or equal to Eq. (20).

The mesh we propose is that away from the corner (between $[\lambda, L_j]$) the mesh is chosen such that it is independent of q_j, while near a corner (between $[0, \lambda]$) the mesh is chosen such that it is independent of L_j. It is reasonable to choose the mesh such that for a fixed N_1:

$$N = \mathcal{O}(N_1 q_j), \text{ between } [0, \lambda]. \quad (21)$$

We now take N, greater or equal to $\hat{c}N_1q_j$, and use Eq. (20) to compute N_{L_j,λ,q_j}, where here $\hat{c}$ is an arbitrary constant. We now define the two meshes:

$$X_j := \tilde{L}_{j-1} + \Lambda_{N,L_j,\lambda,q_j}, \quad Y_j := \tilde{L}_j - \Lambda_{N,L_j,\lambda,q_{j+1}}. \quad (22)$$

This choice of q_j ensures that the approximation error is evenly spread on each mesh interval. Letting $e_\pm(s) := e^{\pm iks}$, $s \in [0, L_j]$, we then define the approximation spaces associated with each mesh as:

$$A_{X_j,\nu} := \{\sigma e_+ : \sigma \in \Pi_{X_j,\nu}\},$$
$$A_{Y_j,\nu} := \{\sigma e_- : \sigma \in \Pi_{Y_j,\nu}\}; \quad (23)$$

for $j = 1, \ldots, n_s$, where

$$\Pi_{X_j,\nu} := \{\sigma \in L^2(0, L_{n_s}) : \sigma|_{(\tilde{L}_{j-1}+x_{m-1}, \tilde{L}_{j-1}+x_m)}$$
$$\text{is a polynomial of degree } \leq \nu,$$
$$\text{for } m = 1, \ldots, N+N_{L_j,\lambda,q_j},$$
$$\text{and } \sigma|_{(0,\tilde{L}_{j-1})\cup(\tilde{L}_j,L)} = 0\},$$
$$\Pi_{Y_j,\nu} := \{\sigma \in L^2(0, L_{n_s}) : \sigma|_{(\tilde{L}_j-y_m, \tilde{L}_j-y_{m-1})}$$
$$\text{is a polynomial of degree } \leq \nu,$$
$$\text{for } m = 1, \ldots, N+N_{L_j,\lambda,q_{j+1}},$$
$$\text{and } \sigma|_{(0,\tilde{L}_{j-1})\cup(\tilde{L}_j,L)} = 0\}; \quad (24)$$

where $\{x_0, \ldots, x_{N+N_{L_j,\lambda,q_j}}\}$ and $\{y_0, \ldots, y_{N+N_{L_j,\lambda,q_{j+1}}}\}$ denote the points of the meshes $\Lambda_{N,L_j,\lambda,q_j}$ and $\Lambda_{N,L_j,\lambda,q_{j+1}}$ respectively. Our approximation space $A_{N,\nu}$ is then the linear span of

$$\bigcup_{j=1,\ldots,n_s}\{A_{X_j,\nu} \cup A_{Y_j,\nu}\}. \quad (25)$$

The number of the degrees of freedom for this problem will be:

$$D_N = 2(\nu+1)\sum_{j=1}^{n_s}(N + N_{L_j,\lambda,q_j}); \quad (26)$$

where the number 2 on the left hand side is due to the fact that we have two meshes Eq. (22), N is the number of points between $[0, \lambda]$ and N_{L_j,λ,q_j} is the number of points between $[\lambda, L_j]$. For our Galerkin Scheme in this paper, we take $\nu = 0$.

Equation (17) is the one we are going to solve for the unknown $\Phi(s)$ by the Galerkin boundary element method. As our starting point we seek:

$$\Phi(s) \approx \Phi_N(s) := \sum_{m=1}^{D_N} v_m \eta_m(s); \qquad (27)$$

where v_m is the unknown coefficient, η_m are the basis functions, and D_N is the total number of basis functions. For $j = 1, \ldots, n_s$, we define n_j^+ and n_j^- to be the number of points of the two meshes X_j and Y_j respectively, so

$$n_j^+ := N + N_{L_j, \lambda, q_j}, \quad n_j^- := N + N_{L_j, \lambda, q_{j+1}}. \qquad (28)$$

We denote the number of points of X_j and Y_j by $s_{j,l}^+$ and $s_{j,l}^-$ respectively, for $j = 1, \ldots, n_s$, $l = 1, \ldots, n_j^{\pm}$. We denote the total number of elements supported on $\cup_{i=1}^{j} \Gamma_i$ by

$$D_{N,j} := \sum_{i=1}^{j} (n_i^+ + n_i^-); \qquad (29)$$

so that the total number of degrees of freedom is $D_N = D_{N,j}$, that is,

$$D_N := \sum_{j=1}^{n} (n_j^+ + n_j^-). \qquad (30)$$

Then, for $j = 1, \ldots, n$, the basis functions are given by

$$\eta_{D_{N,j-1}+j}(s) := \frac{e^{iks}}{\sqrt{s_{j,l}^+ - s_{j,l-1}^+}} \chi_{[s_{j,l-1}^+, s_{j,l}^+)}(s),$$
$$j = 1, \ldots, n_j^+,$$
$$\eta_{D_{N,j-1}+n_j^++l}(s) := \frac{e^{-iks}}{\sqrt{s_{j,l}^- - s_{j,l-1}^-}} \chi_{[s_{j,l-1}^-, s_{j,l}^-)}(s),$$
$$j = 1, \ldots, n_j^-; \qquad (31)$$

where $\chi_{[z_m, z_{m+1})}$ denotes the characteristic function of the interval $[z_m, z_{m+1})$ (z_i, $i = 0, \ldots, D_N$, are the points of each mesh).

4. GALERKIN SCHEME

Substituting Eq. (27) into Eq. (17) and multiplying by a test function $\bar{\eta}_l(s)$ and then integrating over $[0, L]$, gives the following Garlekin scheme (which is a system of linear equations):

$$\sum_{m=1}^{D_N} [(\eta_m, \eta_l) - (\mathcal{K}\eta_m, \eta_l)] v_m = (F, \eta_l). \qquad (32)$$

Now we have to figure out how to compute (η_m, η_l), $(\mathcal{K}\eta_m, \eta_l)$ and (F, η_l). To evaluate these matrices, we follow a similar procedure to that in Langdon and Chandler-Wilde,[11] where most of the formulas are similar. When evaluating the above integrals, we encountered difficulties of dealing with singularities and oscillatory integrals at high frequencies. For the specific problem we are going to discuss here, we encounter the singularities when the basis functions are supported on different side of polygon. When they are supported on the same side

of the polygon, there is hardly any singularity. As such, most of integrals can be evaluated analytically. Ideas dealing with oscillatory integrals is on going research.[12,13] For our problem here, we address the oscillatory integrals by applying standard Gaussian quadrature rule, see Section 5 for detail.

4.1. Evaluation of (η_m, η_l)

The mass matrix will appear in the following form:

$$(\eta_m, \eta_l) = \int_{\mathrm{supp}(\eta_m) \cap \mathrm{supp}(\eta_l)} \frac{e^{(\delta_m - \delta_l)iks}}{\sqrt{(z_{m+1} - z_m)(z_{l+1} - z_l)}} \, ds. \qquad (33)$$

This can be evaluated analytically. Here, $\delta_m = \pm 1$. Notice that, if η_m and η_l are supported on different sides of the polygon, there is no overlap. Hence $(\eta_m, \eta_l) = 0$. If η_m and η_l are supported on the same side of the polygon and $\delta_m = \delta_l$, then there will be total overlap, this forms the diagonal of the whole matrix (η_m, η_l) and in this case $(\eta_m, \eta_l) = 1$. If η_m and η_l are supported on the same side of the polygon and $\delta_m \neq \delta_l$, then there will be some overlaps and non-overlaps. In this case, we integrate between the overlapping intervals. If we define the lower and the upper integrating limits respectively as

$$L_w = \min(z_{l+1}, z_{m+1}) \quad \text{and} \quad U_p = \max(z_l, z_m); \qquad (34)$$

then

$$(\eta_m, \eta_l) = \int_{L_w}^{U_p} \eta_m(s) \bar{\eta}_l(s) ds =$$
$$\frac{e^{-2ikU_p} - e^{-2ikL_w}}{-2ik\sqrt{(z_{m+1} - z_m)(z_{l+1} - z_l)}},$$
$$\text{if} \quad \delta_m = -1 \quad \text{and} \quad \delta_l = 1; \qquad (35)$$

similarly,

$$(\eta_m, \eta_l) = \int_{L_w}^{U_p} \eta_m(s) \bar{\eta}_l(s) ds =$$
$$\frac{e^{-2ikU_p} - e^{-2ikL_w}}{2ik\sqrt{(z_{m+1} - z_m)(z_{l+1} - z_l)}},$$
$$\text{if} \quad \delta_m = 1 \quad \text{and} \quad \delta_l = -1. \qquad (36)$$

4.2. Evaluation of $(\mathcal{K}\eta_m, \eta_l)$

Evaluating this integral is a challenge because it envolves double integrals. It will appear in the following form:

$$(\mathcal{K}\eta_m, \eta_l) = 2 \int_{\mathrm{supp}(\eta_l)} \int_{\mathrm{supp}(\eta_m)} K(s,t) \eta_m(t) \bar{\eta}_l(s) dt \, ds. \qquad (37)$$

If we first consider the case where η_m and η_l are supported on the same side of the polygon, then we see immediately from Eq. (14) that $e_l = e_j$, $f_l = f_j$, $g_l = g_j$, and $h_l = h_j$, hence the term $H_1^{(1)}$ vanishes and Eq. (14) becomes:

$$K(s,t) = -\frac{k}{4} \beta H_0^{(1)}(k|s-t|). \qquad (38)$$

We know from [(12.31)][14] that

$$H_0^{(1)}(s) = \frac{-2i}{\pi} \int_0^\infty \frac{e^{(i-t)s}}{t^{\frac{1}{2}}(t - 2i)^{\frac{1}{2}}} dt, \quad s > 0; \qquad (39)$$

so

$$(\mathcal{K}\eta_m, \eta_l) = -\frac{k\beta}{2} \int_{z_l}^{z_{l+1}} \int_{z_m}^{z_{m+1}} H_0^1(k|s-t|)$$

$$\cdot \frac{\mathrm{e}^{ik(\delta_m t - \delta_l s)}}{\sqrt{(z_{l+1} - z_l)(z_{m+1} - z_m)}} \mathrm{d}t\,\mathrm{d}s =$$

$$\frac{ik\beta}{\pi\sqrt{(z_{l+1} - z_l)(z_{m+1} - z_m)}} \int_0^\infty \frac{J(r)}{r^{\frac{1}{2}}(r - 2i)^{\frac{1}{2}}} \mathrm{d}r; \quad (40)$$

where

$$J(r) = \int_{z_l}^{z_{l+1}} \int_{z_m}^{z_{m+1}} \mathrm{e}^{-rk|s-t| + ik(|s-t| + \delta_m t - \delta_l s)} \mathrm{d}t\,\mathrm{d}s.$$
$$(41)$$

We explore further on how to evaluate Eq. (41), depending on how $[z_l, z_{l+1}]$ and $[z_m, z_{m+1}]$ overlap. In the case where $[z_l, z_{l+1}]$ and $[z_m, z_{m+1}]$ do not overlap, then:

$$J(r) = \left[\frac{\mathrm{e}^{k(i(-\delta_l - 1) + r)z_{l+1}} - \mathrm{e}^{k(i(-\delta_l - 1) + r)z_l}}{k(i(-\delta_l - 1) + r)} \right]$$

$$\cdot \left[\frac{\mathrm{e}^{k(i(\delta_m + 1) - r)z_{m+1}} - \mathrm{e}^{k(i(\delta_m + 1) - r)z_m}}{k(i(\delta_m + 1) - r)} \right]; \quad (42)$$

or

$$J(r) = \left[\frac{\mathrm{e}^{k(i(\delta_l + 1) - r)z_{l+1}} - \mathrm{e}^{k(i(\delta_l + 1) - r)z_l}}{k(i(\delta_l + 1) - r)} \right]$$

$$\cdot \left[\frac{\mathrm{e}^{k(i(\delta_m - 1) + r)z_{m+1}} - \mathrm{e}^{k(i(\delta_m - 1) + r)z_{m+1}}}{k(i(\delta_m - 1) + r)} \right]. \quad (43)$$

In the case where $[z_l, z_{l+1}]$ and $[z_m, z_{m+1}]$ overlap, then Eq. (41) is split further into three integrals:

$$J(r) = \int_{z_l}^{z_m} \int_{z_m}^{z_{l+1}} \mathrm{e}^{-rk(t-s) + ik((t-s) + \delta_m t - \delta_l s)} \mathrm{d}t\,\mathrm{d}s$$

$$+ \int_{z_m}^{z_{l+1}} \int_{z_m}^{z_{l+1}} \mathrm{e}^{-rk|s-t| + ik((|s-t|) + \delta_m t - \delta_l s)} \mathrm{d}t\,\mathrm{d}s$$

$$+ \int_{z_l}^{z_{l+1}} \int_{z_{l+1}}^{z_{m+1}} \mathrm{e}^{-rk(t-s) + ik((t-s) + \delta_m t - \delta_l s)} \mathrm{d}t\,\mathrm{d}s. \quad (44)$$

Computing the first and third integral in Eq. (44) is a straightforward procedure and we can obtain similar formula as those of Eq. (42) or Eq. (43). The second integral of Eq. (44), is a total overlap of δ_m and δ_l (call it $J_a(r)$). Applying exponential power series to this integral leads to Eq. (45) (see top of the next page).

Now we are going to show how to evaluate the integral term:

$$\int_0^\infty \frac{J(r)}{r^{\frac{1}{2}}(r - 2i)^{\frac{1}{2}}} \mathrm{d}r. \quad (46)$$

This appears in Eq. (40). The term in the integral is singular when $r = 0$. In order to remove this singularity, we first change the variables. Let $r = \frac{s^2}{1-s^2}$ then $\frac{dr}{ds} = \frac{2s}{(1-s^2)^2}$, when $r = 0$ implies $s = 0$ and $r = \infty$ implies $s = 1$.

$$\int_0^\infty \frac{J(r)}{r^{\frac{1}{2}}(r - 2i)^{\frac{1}{2}}} \mathrm{d}r =$$

$$\int_0^1 \frac{J(\frac{s^2}{1-s^2})}{(\frac{s^2}{1-s^2})^{1/2}(\frac{s^2}{1-s^2} - 2i)^{1/2}} \frac{2s}{(1-s^2)^2} \mathrm{d}s. \quad (47)$$

Equation (47) appears to be singular at $s = 1$ or $s = 0$, but in fact it is not, since the function $J(r)$ in the numerator composed of exponential functions. Thus, it tends to zero faster then the denominator, as $s \to 1$ or $s \to 0$. We use a standard Gaussian quadrature rule to integrate Eq. (47).

Finally, when η_m and η_l are supported on different sides of the polygon $(\mathcal{K}\eta_m, \eta_l)$, they can only be evaluated numerically, since now $K(s,t)$ cannot be simplified further, which is why we have to use a standard Gaussian quadrature rule.

4.3. Evaluation of (F, η_l)

We shall now evaluate integrals of the form:

$$(F, \eta_l) =$$

$$\frac{1}{\sqrt{z_{l+1} - z_l}} \left[\underbrace{\int_{z_l}^{z_{l+1}} [2f(s) - \Psi(s)]\mathrm{e}^{-ik\delta_l s} \mathrm{d}s}_{I_1} \right.$$

$$\left. - 2 \underbrace{\int_{z_l}^{z_{l+1}} \int_0^L K(s,t)\Psi(t)\mathrm{d}t\,\mathrm{e}^{-ik\delta_l s}\,\mathrm{d}s}_{I_2} \right]. \quad (48)$$

Integral I_1 and some of I_2 can be evaluated analytically while some of I_2 must be computed numerically. When δ_l is supported on Γ_l, we need to consider two cases:

Case1 : If $l \le n_{sh}$ then Γ_l lies in the shadow region and $\Psi(s) = 0$, hence $I_2 = 0$. Thus,

$$I_1 = \int_{z_l}^{z_{l+1}} 2f(s)\mathrm{e}^{-ik\delta_l s}\,\mathrm{d}s =$$

$$2\mathrm{e}^{ik(g_l \sin\theta - h_l \cos\theta)}$$

$$\cdot \left(\frac{\mathrm{e}^{ik(e_l \sin\theta - f_l \cos\theta - \delta_l)z_{l+1}} - \mathrm{e}^{ik(e_l \sin\theta - f_l \cos\theta - \delta_l)z_l}}{ik(e_l \sin\theta - f_l \cos\theta - \delta_l)} \right). \quad (49)$$

Case2 : If $l > n_{sh}$, then Γ_l lies in the illuminated region, thus recalling Eqs. (12) and (15), we have:

$$I_1 = \int_{z_l}^{z_{l+1}} [2f(s) - \Psi(s)]\mathrm{e}^{-ik\delta_l s}\,\mathrm{d}s =$$

$$\int_{z_l}^{z_{l+1}} \frac{2\beta}{\cos\theta' + \beta} u^i(s)\mathrm{e}^{-ik\delta_l s}\,\mathrm{d}s =$$

$$\frac{2\beta\mathrm{e}^{ik(g_l \sin\theta - h_l \cos\theta)}}{\cos\theta' + \beta}$$

$$\cdot \left(\frac{\mathrm{e}^{ik(e_l \sin\theta - f_l \cos\theta - \delta_l)z_{l+1}} - \mathrm{e}^{ik(e_l \sin\theta - f_l \cos\theta - \delta_l)z_l}}{ik(e_l \sin\theta - f_l \cos\theta - \delta_l)} \right). \quad (50)$$

$$J_a(r) = \begin{cases} \frac{e^{-kr(z_{l+1}-z_m)+kr(z_{l+1}-z_m)-1}}{k^2 r^2} + \frac{e^{-k(r-2i)(z_{l+1}-z_m)+k(r-2i)(z_{l+1}-z_m)-1}}{k^2(r-2i)^2}, & \text{if} \quad \delta_l = \delta_m, \\[2ex] \frac{e^{2ikz_{l+1}}}{k(r-2i)}\left[2\left(\frac{e^{-kr(z_{l+1}-z_m)}-1}{kr}\right) - i\left(\frac{1-e^{-2ik(z_{l+1}-z_m)}}{k}\right)\right], & \text{if} \quad \delta_m = 1, \quad \delta_l = -1, \\[2ex] \frac{e^{2ikz_m}}{k(r-2i)}\left[2\left(\frac{e^{-kr(z_{l+1}-z_m)}-1}{kr}\right) - i\left(\frac{1-e^{-2ik(z_{l+1}-z_m)}}{k}\right)\right], & \text{if} \quad \delta_m = -1, \quad \delta_l = 1. \end{cases} \tag{45}$$

$$I_2 = 2\int_{z_l}^{z_{l+1}}\left[\int_{\sum_{m=1}^{n_{sh}}L_m}^{L} K(s,t)\Psi(t)\,dt\right]e^{-ik\delta_l s}\,ds =$$

$$2\sum_{m=n_{sh}+1}^{n_s}\int_{\sum_{p=1}^{m-1}L_p}^{\sum_{p=1}^{m}L_p}\left[\int_{z_l}^{z_{l+1}} K(s,t)e^{-ik\delta_l s}\,ds\right]\Psi(t)\,dt =$$

$$\frac{4\cos\theta'}{\cos\theta'+\beta}$$

$$\cdot\sum_{m=n_{sh}+1}^{n_s}\int_{\sum_{p=1}^{m-1}L_p}^{\sum_{p=1}^{m}L_p}\left[\int_{z_l}^{z_{l+1}} K(s,t)e^{-ik\delta_l s}\,ds\right]u^i(t)\,dt =$$

$$\left[\frac{4\cos\theta'}{\cos\theta'+\beta}\sum_{m=n_{sh}+1}^{n_s}e^{ik(g_m\sin\theta-h_m\cos\theta)}\right]$$

$$\cdot\left[\int_{\sum_{p=1}^{m-1}L_p}^{\sum_{p=1}^{m}L_p}\int_{z_l}^{z_{l+1}} K(s,t)\right.$$

$$\left.\cdot e^{ik((e_m\sin\theta-f_m\cos\theta)t-\delta_l s)}\,dt\,ds\right] =$$

$$\frac{4\cos\theta'}{\cos\theta'+\beta}\sum_{m=n_{shad}+1}^{n}e^{ik(g_m\sin\theta-h_m\cos\theta)}I2_{l,m}. \tag{51}$$

We now evaluate $I2_{l,m}$ when s and t are supported on the same side of the polygon. Recalling Eq. (38),

$$I2_{l,m} =$$

$$\int_{\sum_{p=1}^{m-1}L_p}^{\sum_{p=1}^{m}L_p}\int_{z_l}^{z_{l+1}} K(s,t)e^{ik((e_m\sin\theta-f_m\cos\theta)t-\delta_l s)}\,dt\,ds =$$

$$\frac{-k\beta}{4}\int_{\sum_{p=1}^{m-1}L_p}^{\sum_{p=1}^{m}L_p}\int_{z_l}^{z_{l+1}} H_0^{(1)}(k|s-t|)$$

$$\cdot e^{ik((e_m\sin\theta-f_m\cos\theta)t-\delta_l s)}\,dt\,ds =$$

$$\frac{ik\beta}{2\pi}\int_0^\infty\frac{I^*(r)}{r^{1/2}(r-2i)^{1/2}}\,dr; \tag{52}$$

where

$$I^*(r) = \int_{z_m}^{z_{m+1}}\int_{z_l}^{z_{l+1}} e^{(i-r)k|s-t|+ik(\delta_m t-\delta_l s)}\,dt\,ds; \tag{53}$$

where $z_m = \sum_{p=1}^{m-1}L_p$, $z_{m+1} = \sum_{p=1}^{m}L_p$, $\delta_m = e_m\sin\theta - f_m\cos\theta$. Evaluating Eq. (53) (with a little more effort) leads to Eq. (54) (see top of the next page).

Finally, when s and t are on different side of polygon, we again use the standard Gaussian quadrature rule.
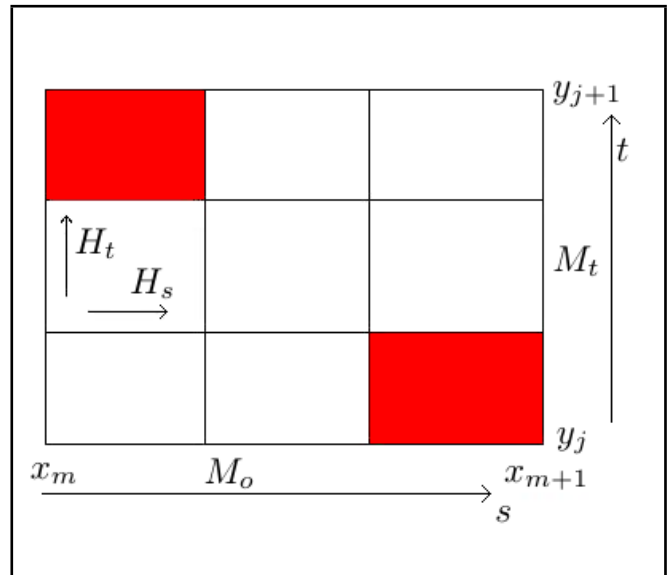

Figure 2. The integrating rectangle.

5. NUMERICAL EVALUATION OF NON-OVERLAPPING INTEGRALS

To evaluate non-overlapping integrals, we first divide the big rectangle $[t_m, t_{m+1}]\times[t_j, t_{j+1}]$ into equally spaced small rectangles with each of sides $H_s\times H_t$, as shown in Fig.2.

In Fig.2, M_s are nodes length between $[t_m, t_{m+1}]$ in the direction s and M_t are nodes length between $[t_j, t_{j+1}]$ in the direction t. Now define

$$H_s := \frac{t_{m+1}-t_m}{M_s}, \qquad H_t := \frac{t_{j+1}-t_j}{M_t}. \tag{55}$$

To deal with the oscillatory nature of integrand, we chose $M_s \propto k$ and $M_t \propto k$. More specifically, we chose $H_t \sim 1/k$ and $H_s \sim 1/k$, then used the two-dimensional Gaussian quadrature rule to approximate each integral on each small rectangle as follows:

$$\int_{t_m}^{t_{m+1}}\int_{t_j}^{t_{j+1}} K(s,t)e^{ik(\sigma_j t-\sigma_m s)}\,dt\,ds =$$

$$\sum_{m=1}^{M_s}\sum_{j=1}^{M_t}\int_{t_m+(m-1)H_s}^{t_m+mH_s}\int_{t_j+(j-1)H_t}^{t_j+jH_t} K(s,t)e^{ik(\sigma_j t-\sigma_m s)}\,dt\,ds =$$

$$\sum_{m=1}^{M_s}\sum_{j=1}^{M_t}\sum_{l=1}^{m_s}\sum_{n=1}^{m_t} w_l w_n K(s_l, t_n)e^{ik(\sigma_j t_n-\sigma_m s_l)}; \tag{56}$$

$$I^*(r) = e^{ik(\delta_m-1)z_m} \left[\frac{e^{ik(1-\delta_l)z_{l+1}+kr(z_m-z_{l+1})} - e^{ik(1-\delta_l)z_l+kr(z_m-z_l)}}{k(r-i(1-\delta_m)k(r-i(1-\delta_l))} \right]$$

$$+ e^{ik(\delta_m+1)z_{m+1}} \left[\frac{e^{-ik(1+\delta_l)z_{l+1}+kr(z_l-z_{m+1})} - e^{-ik(1+\delta_l)z_{l+1}+kr(z_{l+1}-z_{m+1})}}{k(r-i(1+\delta_m)k(r-i(1+\delta_l))} \right]$$

$$+ 2\frac{(e^{ik(\delta_m-\delta_l)z_{l+1}} - e^{ik(\delta_m-\delta_l)z_l})}{ik^2(\delta_m-\delta_l)} \left[\frac{r-i}{\delta_m^2+(r-i)^2} \right]. \quad (54)$$

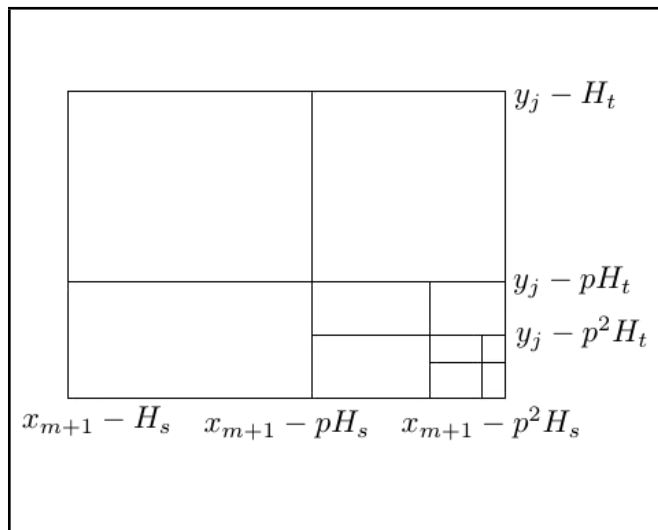**Figure 3.** Removing the singularity.

Figure 4. Behaviour of the solution for increasing k, when $N_1 = 128$.

where m_s and m_t are the number of Gaussian points between $[t_m + (m-1)H_s, t_m + mH_s]$ and $[t_j + (j-1)H_t, t_j + jH_t]$ respectively, and w_l and w_n are weights. We will, however, still have a singularity when the supports of η_j and η_l touch or are close to each other. This situation can occur at the corners of the shaded region shown in Fig.2, that is, when either $t_{m+1} - t_j \leq \epsilon$ or $t_{j+1} - t_m \leq \epsilon$, where $\epsilon > 0$ is a small number close or equal to zero. To deal with this situation, we take the shaded rectangle $[t_{m+1} - H_s, t_{m+1}] \times [t_j, t_j + H_t]$ (the lower bottom) in Fig.2 and subdivide it into small rectangles, with the nodes highly concentrated near the peaked area as shown in Fig.3. We place the nodes at $t_{m+1} - p^l H_s, l = 0, \ldots, n$ (n is the number of Gaussian quadrature points and $p = 0.15$) on $[t_{m+1} - H_s, t_{m+1}]$ and at $t_j + p^l H_t, l = 0, \ldots, n$ on $[t_j, t_j + H_t]$. We again use the two-dimensional Gaussian quadrature rule to approximate each integral on each small rectangle, thus arriving at an equation similar to Eq. (56).

6. NUMERICAL RESULTS

As our numerical example, we take the scattering object Ω, to be a square, with vertices $(0,0)$, $(2\pi, 0)$, $(2\pi, 2\pi)$, and $(0, 2\pi)$. We take $\beta = 1$ on each side Γ_j and the incident angle $\theta = \pi/4$ so that the plane wave is directed towards the corner at $(0, 2\pi)$. The reflective angle in Eq. (15) is given by
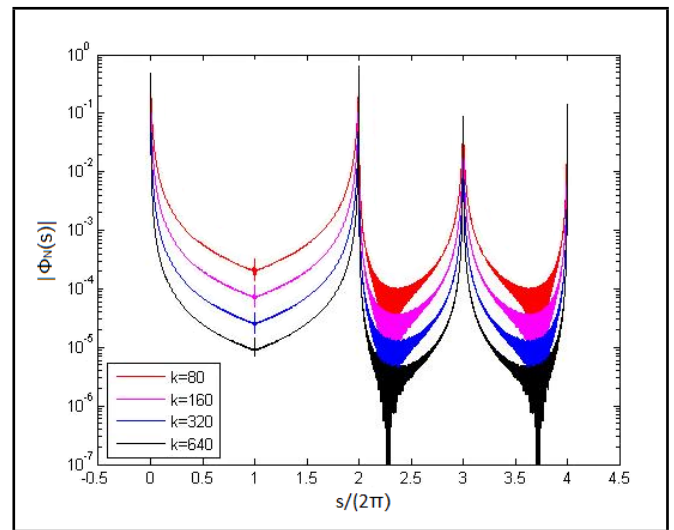
$\theta' = \pi/4$ and $-\pi/4$ in the illuminated regions Γ_3 and Γ_4 respectively. We code the system Eq. (32) to get the unknown v_m and use Eq. (27) to get Φ_N. For this particular example, we chose the mesh such that for a fixed N_1, we use Eq. (21) to compute N, and we use Eq. (20) to compute N_{L_j,λ,q_j}. In Fig. 4 we plot a comparison of the solutions for $N_1 = 128$ for $k = 80, 160, 320$, and 640. As k increases, the diffracted wave decays away faster from the corners. Table 1 shows the errors for fixed $N_1 = 32$ and increasing k. The results in Table 1 shows that errors are inversely proportional to k that is for increasing k the error decreases. This effect is reflected in column $\|\Phi_{128} - \Phi_{N_1}\|_2$ in Table 1. The relative L^2 errors $\|\Phi_{128} - \Phi_{N_1}\|_2 / \|\Phi_{128}\|_2$ remain relatively constant as k increases, which is a good sign for the robustness of our scheme. The degrees of freedom D_{N_1} is proportional to $\log(k)$, that is, D_{N_1} increase logarithmically as the wavenumber increases.

7. CONCLUSIONS

In this paper, we have described how to implement the boundary element method developed in[4] for high frequency scattering by convex polygons with impedance boundary conditions. We explaine in detail how to solve the resulting system of linear equation. We encounter an integration scheme that is frequency independent when we are integrating over elements

Table 1. Relative errors, scattering by square, $N_1 = 32$.

k	D_{N_1}	$\|\Phi_{128} - \Phi_{32}\|_2$	$\|\Phi_{128} - \Phi_{32}\|_2 / \|\Phi_{128}\|_2$
5	376	2.1229×10^{-2}	4.9412×10^{-2}
10	464	1.4873×10^{-2}	4.9022×10^{-2}
20	552	1.0520×10^{-2}	4.9006×10^{-2}
40	640	7.3863×10^{-3}	4.8627×10^{-2}
80	728	5.3551×10^{-3}	4.9871×10^{-2}
160	816	3.6531×10^{-3}	4.8177×10^{-2}
320	904	2.4775×10^{-3}	4.6072×10^{-2}

supported on the same side of the polygon, but our scheme for elements supported on different sides of the polygon has a complicated cost that grows with frequency. For this particular problem, we apply the standard Gaussian quadrature rule in our code to solve such integrals. For our future work, it will be interesting to apply frequency independent schemes for these integrals, such as the ones that have been developed recently by Melenk and Langdon[15] for the problem of scattering by sound soft convex polygons.

REFERENCES

[1] Perrey-Debain, E., Laghrouche, O., Bettess, P., and Trevelyan, J. Plane-wave basis finite elements and boundary elements for three-dimensional wave scattering. *Philosophical Transactions of the Royal Society of London A: Mathematical, Physical and Engineering Sciences*, **362**(1816), 561–577, (2004). http://dx.doi.org/10.1098/rsta.2003.1335.

[2] Perrey-Debain, E., Trevelyan, J., and Bettess, P. Plane wave interpolation in direct collocation boundary element method for radiation and wave scattering: numerical aspects and applications. *Journal of sound and vibration*, **261**(5), 839–858, (2003). http://dx.doi.org/10.1016/S0022-460X(02)01006-4.

[3] Chandler-Wilde, S. N., Graham, I. G., Langdon, S., and Spence, E. A. Numerical-asymptotic boundary integral methods in high frewuency acoustic scattering. *Acta numerica*, **21**, 89–305, (2012). http://dx.doi.org/10.1017/S0962492912000037.

[4] Chandler-Wilde, S., Langdon, S., and Mokgolele, M. A high frequency boundary element method for scattering by convex polygons with impedance boundary conditions. *Communications in Computational Physics*, **11**(02), 573–593, (2012). http://dx.doi.org/10.4208/cicp.231209.040111s.

[5] Mokgolele, M. Numerical solution of high frequency acoustic scattering problems. *PhD Thesis, University of Reading, UK*, , (2009).

[6] McLean, W. C. H. *Strongly elliptic systems and boundary integral equations.* Cambridge university press, (2000).

[7] Colton, D. and Kress, R. *Inverse acoustic and electromagnetic scattering theory*, volume 93. Springer Science & Business Media, (2012). http://dx.doi.org/10.1007/978-3-662-03537-5.

[8] Schenck, H. A. Improved integral formulation for acoustic radiation problems. *The journal of the acoustical society of America*, **44**(1), 41–58, (1968). http://dx.doi.org/10.1121/1.1911085.

[9] Chandler-Wilde, S. N. and Langdon, S. A galerkin boundary element method for high frequency scattering by convex polygons. *SIAM Journal on Numerical Analysis*, **45**(2), 610–640, (2007). http://dx.doi.org/10.1137/06065595X.

[10] Chandler-Wilde, S., Langdon, S., and Ritter, L. A high–wavenumber boundary–element method for an acoustic scattering problem. *Philosophical Transactions of the Royal Society of London A: Mathematical, Physical and Engineering Sciences*, **362**(1816), 647–671, (2004). http://dx.doi.org/10.1098/rsta.2003.1339.

[11] Langdon, S. and Chandler-Wilde, S. Implementation of a boundary element method for high frequency scattering by convex polygons. *Advances in Boundary Integral Methods (Proceedings of the 5th UK Conference on Boundary Integral Methods)*, , 2–11, (2005).

[12] Huybrechs, D. and Vandewalle, S. On the evaluation of highly oscillatory integrals by analytic continuation. *Katholieke Universiteit Leuven, Report TW431*, , (2005).

[13] Huybrechs, D. and Vandewalle, S. The efficient evaluation of highly oscillatory integrals in bem by analytic continuation. *Advances in Boundary Integral Methods, (Proceedings of the 5th UK Conference on Boundary Integral Methods)*, , 12–21, (2005).

[14] Abramowitz, M., Stegun, I. A., et al. Handbook of mathematical functions. *Applied mathematics series*, **55**, 62, (1966).

[15] Melenk, J. M. and Langdon, S. An hp-bem for high frequency scattering by convex polygons. *Proc. 8th Int. Conf. on Mathematical and Numerical Aspects of Wave Propagation, Reading University*, , 93–95, (2007).